Society For Biomaterials

Cell shape and the presentation of adhesion ligands guide smooth muscle myogenesis

Douglas Zhang, Michael B. Sun, Junmin Lee, Amr A. Abdeen, Kristopher A. Kilian

Department of Materials Science and Engineering, University of Illinois at Urbana-Champaign, Urbana, Illinois

Received 10 September 2015; revised 7 January 2016; accepted 19 January 2016
Published online 11 February 2016 in Wiley Online Library (wileyonlinelibrary.com). DOI: 10.1002/jbm.a.35661

Abstract: The reliable generation of smooth muscle cells is important for a number of tissue engineering applications. Human mesenchymal stem cells (MSCs) are a promising progenitor of smooth muscle, with high expression of smooth muscle markers observed in a fraction of isolated cells, which can be increased by introduction of soluble supplements that direct differentiation. Here we demonstrate a new micropatterning technique, where peptides of different ligand affinity can be microcontact printed onto an inert background, to explore MSC differentiation to smooth muscle through controlled biochemical and biophysical cues alone. Using copper-catalyzed alkyne-azide cycloaddition (CuAAC), we patterned our surfaces with RGD peptide ligands—both a linear peptide with low integrin affinity and a cyclic version with high integrin affinity—for the culture of MSCs in shapes with various aspect ratios. At low aspect ratio, ligand affinity is a prime determinant for smooth muscle differentiation, while at high aspect ratio, ligand affinity has less of an effect. Pathway analysis reveals a role for focal adhesion turnover, Rac1, RhoA/ROCK, and calpain during smooth muscle differentiation of MSCs in response to cell shape and the affinity of the cell adhesion interface. Controlling integrin-ligand affinity at the biomaterials interface is important for mediating adhesion but may also prove useful for directing smooth muscle myogenesis. Peptide patterning enables the systematic investigation of single to multiple peptides derived from any protein, at different densities across a biomaterials surface, which has the potential to direct multiple MSC differentiation outcomes without the need for soluble supplements. © 2016 Wiley Periodicals, Inc. J Biomed Mater Res Part A: 104A: 1212–1220, 2016.

Key Words: mesenchymal stem cells, microcontact printing, peptides, smooth muscle, self-assembled monolayers

How to cite this article: Zhang D, Sun MB, Lee J, Abdeen AA, Kilian KA. 2016. Cell shape and the presentation of adhesion ligands guide smooth muscle myogenesis. J Biomed Mater Res Part A 2016:104A:1212–1220.

INTRODUCTION

Smooth muscle cells (SMCs) are found within the walls of blood vessels and multiple other tissues. Their primary function involves contraction and they serve important roles during vascular development. Functional smooth muscle cells are thereby critical for cell-based therapies involving vasculogenesis and vascular diseases.[1] Mesenchymal stem cells (MSCs) serve as an attractive cell source for smooth muscle due to their relative ease of acquisition and culture[2] compared with SMCs.[3] Whereas vascular smooth muscle cells are typically derived by removing the endothelial layer of blood vessels to extract the underlying sheets of smooth muscle cells,[4] MSCs can be acquired from a wide variety of cell sources and separated through simple isolation procedures[5] for expansion and differentiation to a smooth muscle phenotype.

MSCs have been shown to commit to a wide array of lineages through control of biophysical and biochemical properties including cell geometry,[6–8] substrate rigidity,[9] and matrix composition.[10,11] Heterogeneous populations of isolated MSCs will contain a fraction of cells that express SMC markers, and there are several microenvironment factors that are believed to contribute to the SMC phenotype including soluble factors, extracellular matrix components, and physical cues.[12] MSCs have been differentiated into SMCs via direct treatment with TGFβ,[13] PDGF,[14] and a variety of other biocompounds.[12] Direct interaction with the extracellular matrix (ECM) has been shown to be equally important in promoting smooth muscle phenotypes. Early reports have demonstrated that fibronectin, typically found in serum and used to coat culture substrates, supported a loss of the SMC contractile phenotype[15] whereas basement membrane proteins such as laminin and Type IV collagen could delay this transition.[16] Another study demonstrated that exposing MSCs to endothelial cell matrix[17] could induce those cells to differentiate toward a SMC phenotype. Likewise the mechanical environment has also been shown to be important in determining SMC phenotype. Researchers have demonstrated how MSCs respond to mechanical stimulation through compressive strain[18] and alignment[19] to guide specification of markers associated with the smooth muscle phenotype. Combinatorial tools that can explore the interplay

Additional Supporting Information may be found in the online version of this article.
Correspondence to: K. A. Kilian; e-mail: kakilian@illinois.edu
Contract grant sponsor: National Heart Lung and Blood Institute; contract grant number: HL1,2,1757
Contract grant sponsor: National Science Foundation; contract grant number: CBET 14–54,616 CAR

between ligand presentation and mechanical stimulation offer an attractive method to decouple the complex mechanisms that modulate SMC differentiation and phenotypic behavior.

Microcontact printing of self-assembled monolayers (SAMs) is a widely used tool that allows manipulation of the biophysical and biochemical properties of cell culture materials. Traditionally self-assembled monolayers are produced using long-chain alkanethiolates that are patterned onto a gold surface,[20,21] followed by passivation of the intervening regions, and location-specific adsorption of an ECM protein such as fibronectin, collagen, or laminin. Although long-chain ECM molecules are useful for promoting cellular adhesion, these proteins are known to contain multiple binding domains and configurations. Depending on the local environment, these proteins can exist in different conformations, have binding sites buried or exposed, or interact with synergistic and antagonistic local domains.[22,23] Smooth muscle in particular, is known to be sensitive to ECM properties, where differentiation and maintenance of a contractile phenotype is affected by the protein components[12,17] and local environment.[13] These interactions between cell and substrate can be biochemical as well as mechanical. Environmental cues such as stiffness and topography, and changes in adhesion ligands or restriction of cell size, all affect the contractility of actin and its motor myosin II, to direct cells to undergo specific processes.

In this article we present an alternative approach to conventional microcontact printing, where incorporation of an azido-terminated alkanethiolate into the printing solution enables patterning of specific peptides on the surface of our SAMs. The use of short peptides for surface modification presents several advantages over the use of whole proteins. Peptides are cost-efficient, easy to synthesize and purify, and able to be conjugated in a spatially defined manner.[24] Furthermore, short peptides presented on inert backgrounds allow the unambiguous study of discreet ligand-receptor interactions. We demonstrate how subtle changes in peptide presentation, from a linear to a cyclic variant of RGD, will influence focal adhesion dynamics and the differentiation of MSCs toward a smooth muscle phenotype. We examine the interplay between ligand–integrin affinity and cell geometry and find that changing the aspect ratio of single cells will influence the spatial guidance of focal adhesions, and that intracellular signaling pathways respond to shape and ligand differently.

MATERIALS AND METHODS

Materials

Glass coverslips were purchased from Fisher Scientific. All chemicals were purchased from Sigma Aldrich unless noted otherwise. The 11-(2-{2-[2-(2-azido-ethoxy)-ethoxy]-ethoxy}-ethoxy)-undecane-1-thiol (referred to as HS-C11-EG4-N3) was purchased from Prochimia (Sopot, Poland, TH 008-m11.n4–0.2). Triethylene glycol mono-11-mercaptoundecyl ether (referred to as HS-C11-EG3) was purchased from Sigma Aldrich (673,110). Tissue culture plasticware was purchased from Fisher Scientific. Peptide synthesis reagents and amino acids were purchased from Anaspec. Cell culture media and reagents were purchased from Gibco. Human mesenchymal stem cells (hMSCs) were purchased from Lonza and produced by Osiris Therapeutics. These cells were derived from bone marrow isolated from the iliac crest of human volunteers.

Peptide synthesis

The peptide sequence GRGDS was synthesized manually by standard Fmoc solid-phase methodology as previously described.[11] The synthesized peptide was purified (>90%) using reversed-phase high-performance liquid chromatography (RP-HPLC) (Perkin-Elmer Flexar) with a C18 column (Waters). The cyclic peptide RGD{d-Phe}{propargyl-Gly} was purchased from Genscript (>90%) and used as received.

Surface preparation

Surfaces were fabricated by electron beam evaporation of 5 nm of Ti followed by 20 nm of Au onto cleaned glass coverslips, followed by storage in a desiccator for up to 1 week. To pattern, polydimethylsiloxane (PDMS, Polysciences) stamps were fabricated by polymerization upon a patterned master of photoresist (SU-8, MicroChem) created using UV photolithography through a laser printed mask. Stamps featuring four different patterns (circular 1:1, oval 1:2, oval 1:4, oval 1:8) of 3000 μm^2 were used. Stamps were inked with the inking solution consisting of 15 mol % HS-C11-EG4-N3, 85 mol % HS-C11-EG3 in ethanol (1 m*M* total), dried under air, and applied to the surface of the gold. Surfaces were then rinsed with ethanol, dried, and incubated overnight with 1mM HS-C11-EG3 in ethanol to prevent nonspecific adsorption to non-patterned regions.

Peptide conjugation

Stock solution of linear and cyclic peptide ligand (1 m*M* in H_2O) and Tris[(1-benzyl-1*H*−1,2,3-triazol-4-yl)methyl]amine (TBTA) [10 m*M* in DMSO/t-butyl alcohol (3:1)] were aliquoted and stored at −20°C. Copper solution (10 m*M* Cu, 10 m*M* sodium ascorbate in DMSO) was prepared fresh prior to azide-alkyne cycloaddition. Click solution was prepared by combining stock TBTA solution with fresh Cu solution (2:1 v/v). Reaction mixtures containing peptide ligand (5 μL) and click solution (5 μL) were prepared and reacted with patterned surfaces overnight at room temperature. The surfaces were then placed into 24-well plates, rinsed 2× with DI water, incubated with 50mM EDTA for 5 min to remove residual copper, and finally rinsed 3× with DI water followed by ethanol.

Cell culture

Human mesenchymal stem cells (hMSCs) were cultured in Dulbecco's Modified Eagle's Medium (DMEM) low glucose (1 g mL^{-1}) media supplemented with 10% fetal bovine serum (MSC approved FBS; Invitrogen), 1% penicillin/streptomycin, media changed every 3–4 days and passaged at ~80% confluency using 0.25% Trypsin:EDTA (Gibco). MSCs were seeded on patterned and non-patterned surfaces at a cell density ~20,000 cells cm^{-2} and cultured for 5 days before fixing. For pharmacological inhabitation studies, we used Blebbistatin (10 μ*M*), Y27632 (10 μ*M*), Calpain Inhibitor I (130 μ*M*, Sigma A6185), and Rac Inhibitor II (50 μ*M*, CAS 109 0893–12–1,

Calbiochem). MSCs were tested for purity by Lonza, and were positive for CD105, CD166, CD29, and CD44, negative for CD14, CD34, and CD45 by flow cytometry, and had ability to differentiate into osteogenic, chondrogenic, adipogenic lineages (http://www.lonza.com). The use of human MSCs in this work was reviewed and approved by the University of Illinois at Urbana-Champaign Biological Safety Institutional Review Board.

Immunocytochemistry

Cells were fixed with 4% paraformaldehyde (PFA) for 20 min, permeabilized with 0.1% Triton X-100 in PBS for 20 min, and blocked with 0.1% bovine serum albumin (BSA) in PBS for 30 min. Primary antibody labeling was performed in 5% goat serum containing 0.1% BSA in PBS overnight at 4°C with rabbit anti-paxillin (1:200 dilution, abcam ab3,2084), mouse anti-$\alpha_5\beta_1$ (1:200 dilution, Millipore MAB1969), mouse anti-$\alpha_v\beta_3$ (1:200 dilution, Millipore MAB1976Z), mouse anti-αSMA (1:200 dilution, abcam ab7817). Secondary antibody labeling was performed similarly with Alexa Fluor 488-conjugated anti-rabbit IgG antibody and Alexa Fluor 647-conjugated anti-mouse IgG antibody (1:500 dilution) along with Texas Red-conjugated phalloidin (1:200 dilution) and DAPI (1:5000 dilution) for 1 h at room temperature. Surfaces were fixed on glass slides using Prolong Gold Antifade (Thermo Fisher) and imaged with an INCell Analyzer 2000 (GE).

RNA isolation and RT-PCR

MSCs were cultured on linear and cyclic-RGD presenting SAMs for 24 h. Adherent cells were lysed with TRIzol reagent (Invitrogen) and total RNA was isolated by chloroform extraction and ethanol precipitation. Total RNA in DEPC water was amplified using TargetAmp 1-Round aRNA Amplification Kit 103 (Epicentre) according to vendor protocols. Total RNA was reverse transcribed using Superscript III First Strand Synthesis System for RT-PCR (Invitrogen). RT-PCR was performed linearly by cycle number for each primer set using SYBR Green RealTime PCR Master Mix (Invitrogen) on an Eppendorf Realplex 4S Real-time PCR system. Primer sequences were as follows (forward and reverse):

α5: TGCCGAGTTCACCAAGACTG and TGCAATCTGCTCCTG AGTGG

αv: CATCTTAATGTTGTGCCGGATGT and TCCTTCCACAATC CCAGGCT

β1: CCGCGCGGAAAAGATGAATTT and AGCAAACACACAGC AAACTGA

β3: TTGGAGACACGGTGAGCTTC and GCCCACGGGCTTTAT GGTAA

GAPDH: TGCCTCGATGGGTGGAGT and GCCCAATACGACCA AATCAGA

Image analysis

Immunofluorescent images were analyzed using ImageJ software. To count α-SMA positive and negative cells, the channel staining for α-SMA was overlayed over the nuclei channel. Nuclei that stained positive for α-SMA was counted manually and subtracted from the total number of nuclei. For patterned cells, only cells conforming to the pattern shapes were chosen for analysis. For heat maps, cells were overlayed and a z-projection was taken for the average intensity. Masks of heat maps were generated by normalizing the backgrounds and thresholding the results of the z-projection. At least two independent experiments with triplicate samples were performed to verify results. To calculate p values, the results of all experiments were pooled and a Fisher's exact test was performed on the ratios of α-SMA$^+$ cells using GraphPad software.

RESULTS

Patterning peptide derivatized self-assembled monolayers on gold surfaces

We found that an ethanoic solution containing an azido-terminated tetra(ethylene glycol) alkanethiolate (HS-C11-EG4-N3) could be micropatterned similar to traditional long-chain alkanthiolates. Self-assembled monolayers patterned this way supported cell adhesion in defined geometries for >2 weeks in culture (Supporting Information Fig. S1). After backfilling non-patterned areas with a tri(ethylene glycol) alkanethiolate to resist non-specific protein adsorption (HS-C11-EG3), surfaces can be further modified with alkyne-containing peptides using copper-catalyzed alkyne-azide cycloaddition (CuAAC) to generate well defined geometries of peptide-adhesion ligands (Fig. 1). Importantly, patterning the nonadhesive RDG peptide resulted in negligible cell adhesion (data not shown). We investigated four geometries with varying aspect ratios and used a low affinity linear version and a high affinity cyclic version of the RGD peptide[25,26] to investigate the combined effect of ligand affinity and geometry on the differentiation of MSCs toward a smooth muscle phenotype.

Mesenchymal stem cell phenotype changes on peptide-presenting SAMs

MSCs cultured on the linear and cyclic RGD peptide surfaces exhibited differences in cell spread area (Fig. 2). We immunostained the MSCs for α-smooth muscle actin (αSMA), a key marker of smooth muscle differentiation, and found that a higher fraction of MSCs cultured on the cyclic RGD peptide expressed αSMA when compared with MSCs cultured on linear RGD (Fig. 2). This trend was consistent for up to 10 days in culture. The differences in cell size was also accompanied by changes in the focal adhesion architecture in the adherent cells. MSCs cultured on cyclic RGD displayed smaller focal adhesion complexes [Fig. 3(a,b)], with an increased average number of focal adhesions per cell, although this result was not significant ($P = 0.07$). These observations are consistent with earlier reports of smaller focal adhesions and higher focal adhesion turnover for cells cultured on cyclic RGD, compared with linear RGD where cells adopt larger, more stable focal adhesions at the perimeter.[27] Interestingly, we also noticed differences in integrin expression between MSCs cultured on the two peptides. We immunostained for $\alpha_5\beta_1$ and $\alpha_v\beta_3$ integrin, receptors that are commonly expressed in MSCs and can adhere to a variety of RGD-based peptide motifs,[28] and observed no significant changes in $\alpha_5\beta_1$ expression between MSCs cultured on the linear or cyclic variant of RGD. However, we detected significantly higher $\alpha_v\beta_3$ integrin expression when MSCs were cultured on the cyclic peptide

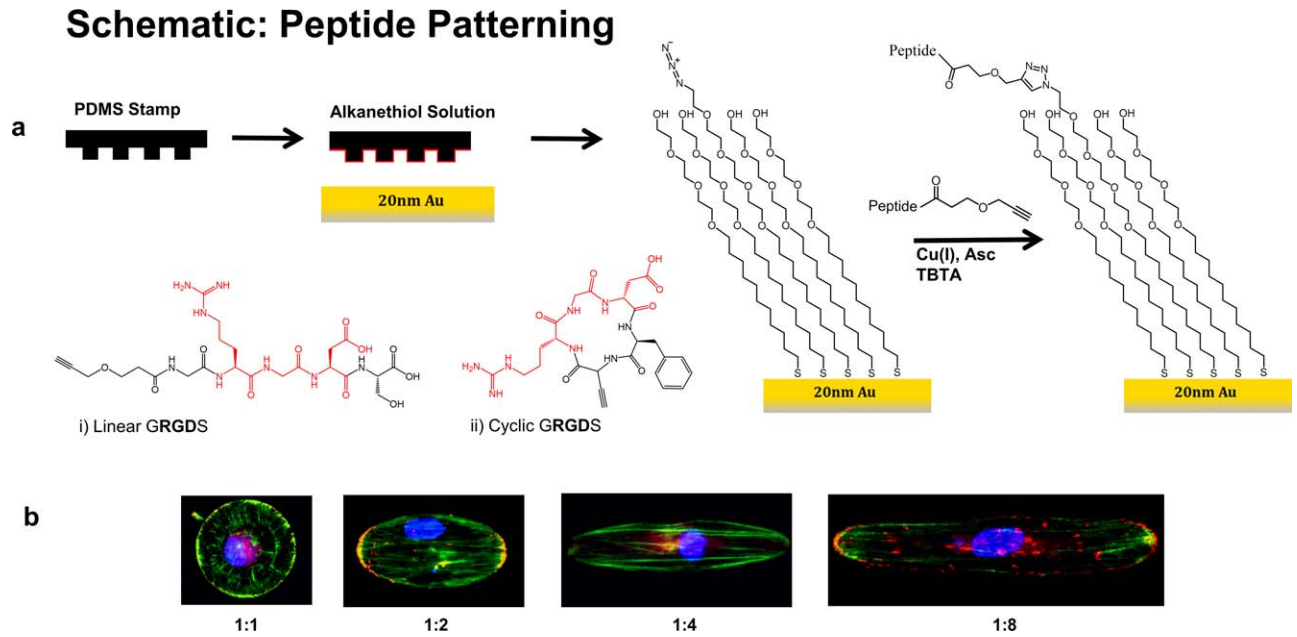

FIGURE 1. Azido-terminated monolayers were patterned on gold using microcontact printing. (a) A linear (low affinity) RGD peptide and cyclic (high affinity) RGD are then conjugated to the surfaces of the patterned substrates using copper-catalyzed azide-alkyne cycloaddition. (b) Four geometries were investigated with the same area (3000 μm^2) but varying aspect ratios. Representative cells cultured on linear RGD patterns are shown. Blue = Nuclei, Red = Paxillin, Green = F-Actin.

[Fig. 3(c)]. We also measured initial integrin mRNA expression of MSCs 24 h after adhering to the peptide surfaces. We observe that MSCs adhering to linear RGD express higher levels of α_5 integrin, while MSCs adhering to cyclic RGD express slightly higher levels of α_v integrin [Fig. 3(d)]. Previous investigations have shown that a bent conformation of the RGD sequence presents a closer fit to the $\alpha_v\beta_3$ receptor and leads to improved ligand binding.[29] Our own observations then seem to

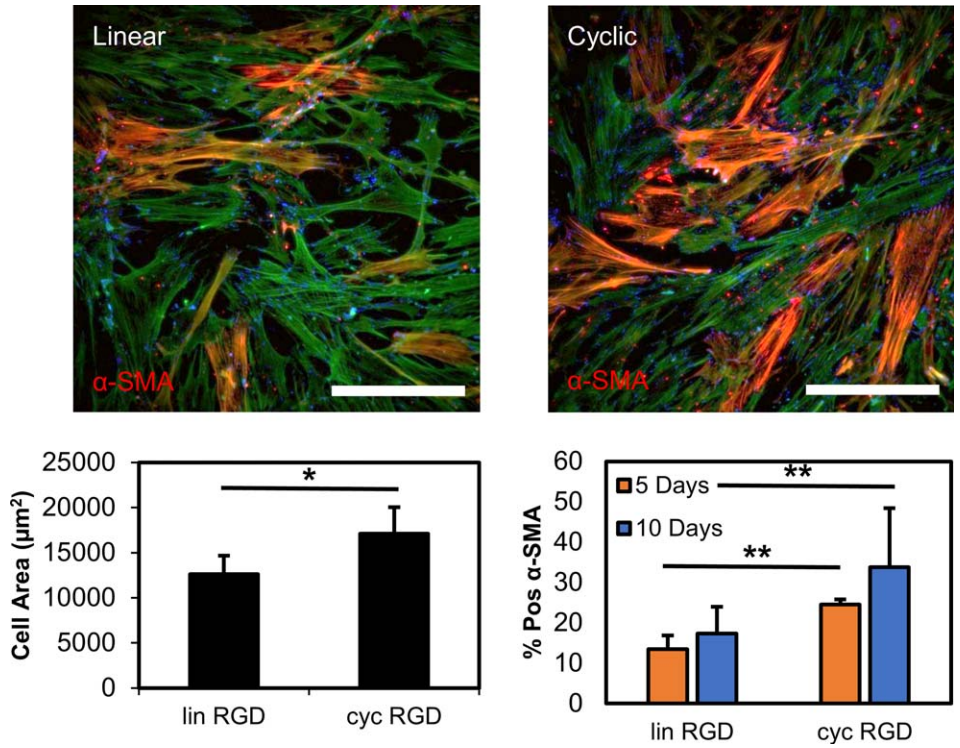

FIGURE 2. MSCs cultured on linear and cyclic RGD peptide display phenotypic differences in cell spread area after 5 days, and a greater percentage of cells express α-smooth muscle actin when cultured on the cyclic peptide. Blue = Nuclei, Red = α-smooth muscle actin, Green = F-Actin. Error bars show SD between two independent experiments with three replicates each. *p* values calculated using Fisher's exact test for %positive α-SMA, * $p < 0.05$, ** $p < 0.01$. Scale bar = 200 μm.

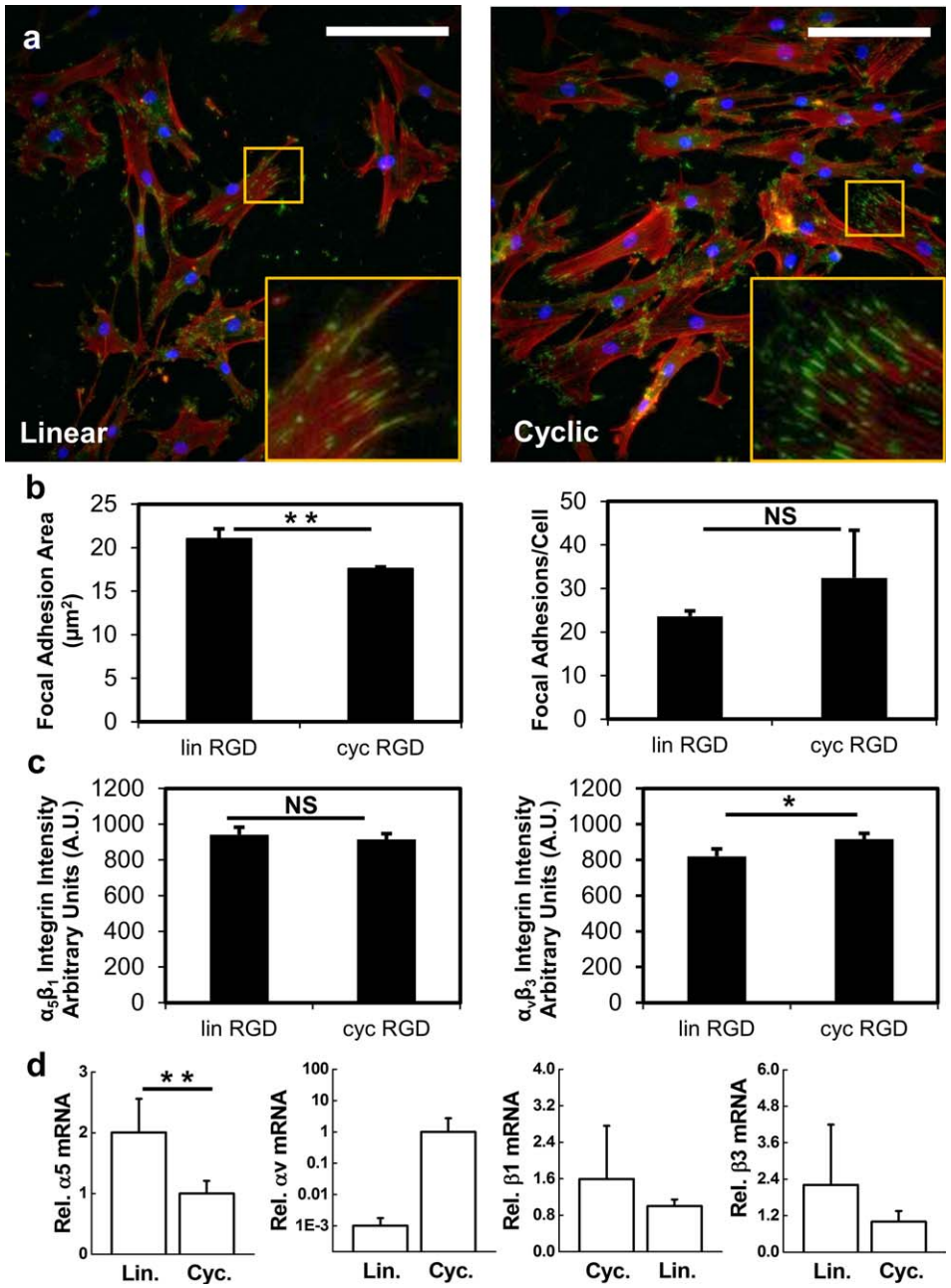

FIGURE 3. Differences in focal adhesion architecture between MSCs cultured on linear and cyclic RGD. (a,b) Linear RGD promotes larger individual focal adhesion complexes, while MSCs on cyclic RGD have on average more focal adhesions per cell. (c) Integrin expression was quantified via immunofluorescence staining after 5 days of culture on RGD presenting surfaces. (d) Initial integrin mRNA expression after 24 h is also assessed via RT-PCR. Blue = Nucleii, Red = F-Actin, Green = Paxillin. Error bars show SD between two independent experiments. p values calculated using two-tailed student t test, * $p < 0.05$, ** $p < 0.01$. Scale bar = 200 μm.

suggest that not only is there an effect of ligand affinity, but differences in peptide conformation can also lead to overall differences in integrin expression. Because differences in cell spreading are well known to affect downstream signaling,[6,7] we employed our peptide patterning approach to normalize cell spread area and to investigate how αSMA expression changes with cell shape.

First we explored how controlling cell geometry may influence the number and size of focal adhesions on the cyclic or linear peptides. Heat maps of paxillin-stained patterned cells at one (Supporting Information Fig. S2) and 5 days show uniform focal adhesions at the perimeter, with a larger focal adhesion footprint throughout the body of the cell on cyclic peptide surfaces [Fig. 4(a)]. This is consistent with our earlier work[30] as well as the work of other groups who report on average more focal adhesions per cell on cyclic RGD.[27] As aspect ratio is increased we observe focal adhesion localization toward the extreme axes of the cells. Previous studies have demonstrated stabilization of focal adhesions to the short ends of the cell as aspect ratio is increased to stabilize actin filaments along the

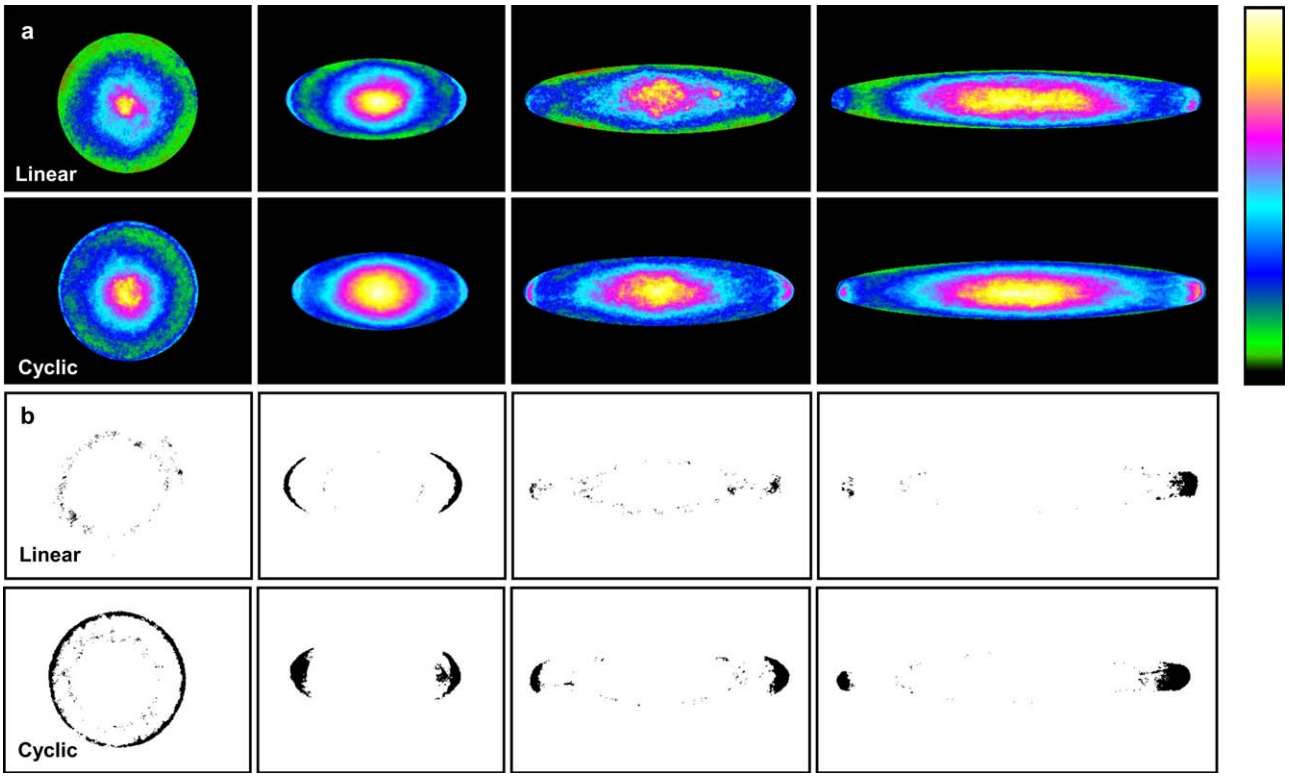

FIGURE 4. Heat maps of paxillin localization of MSCs cultured on linear and cyclic RGD peptide. (a) As aspect ratio increases, focal adhesions become localized toward the cell poles. (b) Mask of focal adhesion intensity shows changes in focal adhesion size and footprint between linear and cyclic peptide.

long edge of the cell through myosin II generated tension.[31] From our paxillin-stained heatmaps, we are able to generate a mask to show the focal adhesion footprint along the periphery in each condition. We observe similar average intensity of paxillin (data not shown) across all samples, but differences in the "footprint" of how the focal adhesions are distributed. As aspect ratio increases, the focal adhesion footprint becomes larger and more localized toward the periphery of the cell.

When we confine the cells to keep spread area constant and increase the aspect ratio, we continue to observe a pattern where the cyclic peptide promotes higher αSMA expression in all geometries, with the greatest difference occurring at the 1:4 aspect ratio [Fig. 5(a)]. Interestingly, as the aspect ratio is increased to 1:8, the difference in αSMA expression between linear and cyclic peptides is reduced and non-significant at a p values of 0.05. We also observe an interesting trend in αSMA expression and the focal adhesion footprint. For each aspect ratio, cells patterned on cyclic RGD tended to have a greater footprint area than cells on linear RGD, with the highest differences in the 1:1 isotropic ratio ($p = 0.08$), and the 1:4 ratio ($p < 0.05$) [Fig. 4(b)]. At 1:4 aspect ratio, where there is the most significant difference in αSMA expression due to the peptide alone, there is also the greatest difference in the focal adhesion footprint between the cells [Fig. 5(b)]. At a 1:8 aspect ratio, where the difference in αSMA expression is less significant, there is also very little difference in focal adhesion distribution between this condition, highlighting the importance of focal adhesion architecture in differentiation processes. However, while αSMA expression is normalized between different affinity peptides as aspect ratio is increased, total expression of αSMA increases.

Pharmacological inhibition of mechanotransduction pathways

Given the differences in focal adhesions, we examined several protein targets that are known to be involved in focal adhesion architecture and turnover. We focused on the 1:1 isotropic pattern and the 1:4 aspect ratio pattern as these seemed to be the geometries that elicited the most significant differences in α-SMA expression. We investigated Rac1, a well-characterized GTPase which drives membrane protrusion and formation of nascent focal complexes,[32] non-muscle myosin II, a central protein involved in many cell migration and adhesion pathways,[33] Rho-associated, coiled coil-containing kinase (ROCK), an upstream regulator of myosin II,[34] and calpain, a protein involved in various biological processes, including migration and cytoskeletal remodeling.[35,36]

Rac is a type of Rho GTPase known to play an important role in adhesion dynamics.[31] Rac1 is particularly interesting as it has been previously shown to be involved in smooth muscle differentiation of MSCs.[37] However, after treating MSC cultures with an inhibitor of Rac1, we found no significant differences in α-smooth muscle expression at the 1:1 and 1:4 aspect ratios (Fig. 6). We also use inhibitors of actomyosin contractility—blebbistatin to inhibit myosin II, and Y-27632 to inhibit ROCK—and see variable responses. At low aspect

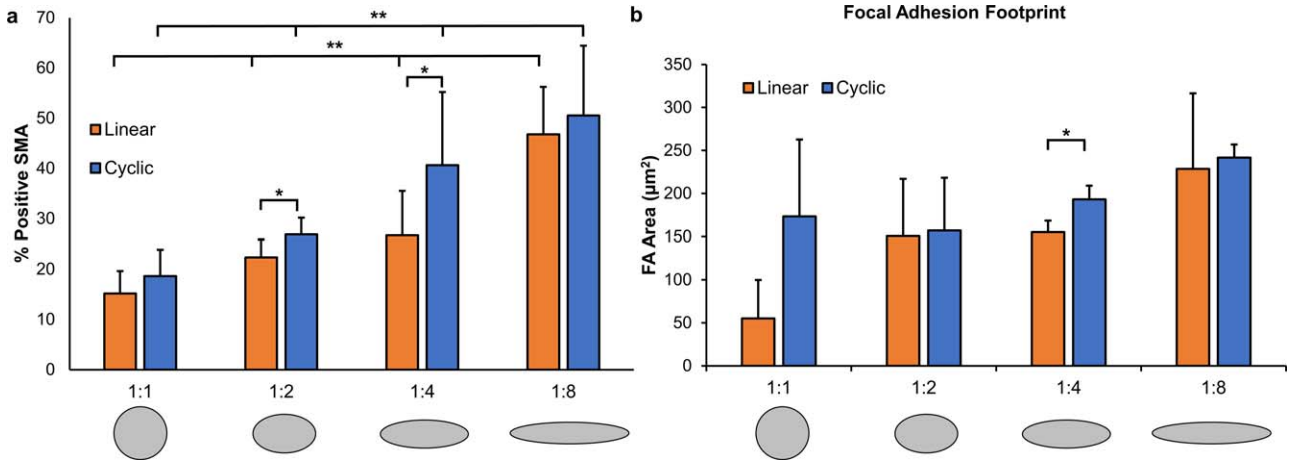

FIGURE 5. MSCs are cultured in patterns presenting either a linear or cyclic variant of RGD. (a) After 5 days, patterns with higher aspect ratios contained significantly more cells expressing α-smooth muscle actin. The cyclic peptide, known to have higher affinity for the αvβ3 integrin also promotes higher α-smooth muscle actin expression compared with the linear peptide. Differences in expression levels are the most significant at intermediate aspect ratios (1:2 and 1:4). (b) On the basis of masks of focal adhesion footprints at each aspect ratio, we see the most significant changes in overall area of focal adhesion localization at a low isotropic 1:1 aspect ratio, and an intermediate 1:4 aspect ratio. Error bars show SEM between three independent experiments with three replicates each. *p* values calculated using Fisher's exact test, * $p < 0.05$, ** $p < 0.01$.

ratio, we see no significant effect of either myosin II or ROCK inhibition. However at a high 1:4 aspect ratio, we observe ~50% decreases in αSMA expression on both linear and cyclic peptides. Calpain, a less studied protease has also emerged as an important mediator of focal adhesion disassembly and turnover.[38] When treated with a calpain inhibitor, we observe a significant decrease in αSMA expression in cells cultured on both linear and cyclic peptide substrates, only when patterned at high aspect ratio (Fig. 6).

DISCUSSION

We present a technique that allows precise control over both ligand presentation and cell geometry and demonstrate that even a small change in ligand presentation (linear vs. cyclic) can significantly affect the differentiation of MSCs to a smooth muscle phenotype. A cyclic conformation of the RGD pentapeptide containing a hydrophobic d-amino acid at the i + 1 position of the βII′-turn and glycine at the i + 1 position of the γ-turn has been known to more closely resemble the loop domain of vitronectin and fibrinogen that binds to the $\alpha_v\beta_3$ heterodimer, and has greater specificity and selectivity in binding to this integrin compared with linear RGD peptides.[29] Previous work has shown cyclic RGD to have greater selectivity toward the $\alpha_v\beta_3$ integrin and its downstream signaling pathways.[25,26,39,40] In support of these studies, we see increased expression of the $\alpha_v\beta_3$ integrin on MSCs cultured on the cyclic peptide, with slightly higher $\alpha_5\beta_1$ in MSCs cultured on the linear peptide. There is a similar trend in MSC integrin expression at both the initial mRNA level, and at the protein level via immunofluorescence after 5 days, although we note that statistical significance varied across these experiments. We believe these differences may be on account of the techniques as well as subtle changes in integrin expression over time. Nevertheless, we believe these experiments support the role of αvβ3 expression in MSCs cultured on the

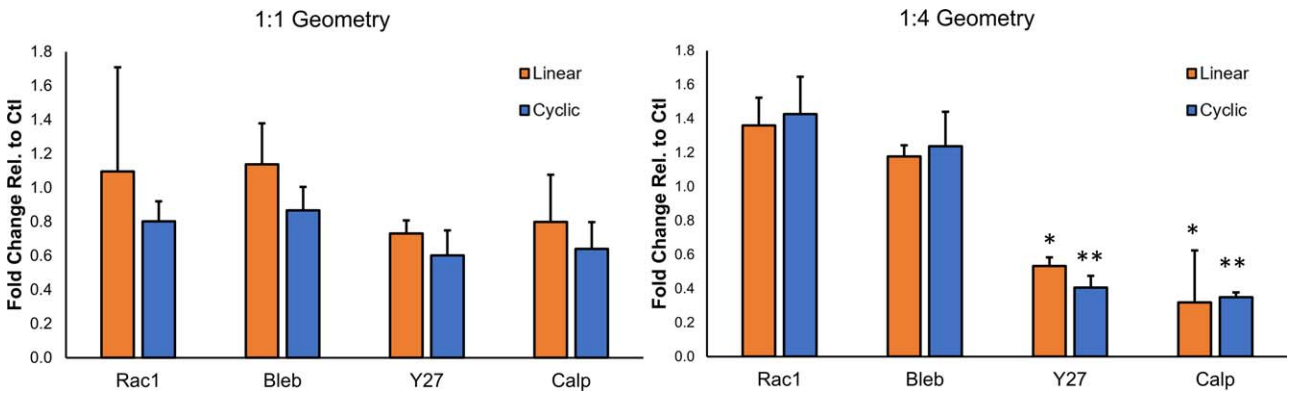

FIGURE 6. Several protein targets that are known to be involved in focal adhesion architecture and turnover are knocked down using pharmacological inhibition. We see marked changes in expression of α-smooth muscle actin with respect to untreated control MSCs. At a low isotropic aspect ratio (1:1) geometry, we see slight decreases in expression with addition of Y27632 (ROCK inhibitor), and Calpain I inhibitor, though these effects were not significant. However, at high aspect ratio (1:4), we see a significant decrease in expression upon ROCK and Calpain inhibition. Error bars show SEM between two independent experiments. *p* values calculated using student's *t* test between replicate samples, * $p < 0.05$, ** $p < 0.01$.

cyclic peptide. We also observe a similar effect as has been reported by Kato and Mrksich where MSCs cultured on the linear peptide had larger focal adhesions, while MSCs on cyclic RGD had a greater number of smaller focal adhesions.[27] Because our platform presents the RGD peptide in a controlled density and orientation, we presume that phenotypic changes are influenced largely by the affinity of the ligand for integrin receptors.

Because cellular elongation has been demonstrated to influence the smooth muscle phenotype,[19] we next explored how altering the aspect ratio of single cells influence the interactions of MSCs with these ligands of different affinity. Interestingly, the effects of RGD cyclization seem to be most pronounced at 1:4 intermediate aspect ratio. While cyclic RGD patterned MSCs express more αSMA than linear RGD patterned MSCs at all aspect ratios, the effects are most significant at an aspect ratio of 1:2 and 1:4. The 1:4 aspect ratio is also where we observe the greatest difference in the focal adhesion architecture of individually patterned cells. Masks of focal adhesion heat maps show that in MSCs cultured on cyclic RGD, paxillin-stained focal adhesions have a larger "footprint" than on linear RGD. This corresponds with previous observations that cyclic RGD promotes smaller focal adhesions and more rapid turnover, whereas linear RGD promotes larger more stable focal adhesions. As cell aspect ratio is increased to 1:8 we see the highest αSMA expression, but with attenuation of the influence of ligand affinity, which suggests elongation of the cell dominates the smooth muscle phenotype.

Treatment of MSCs with blebbistatin, an inhibitor of myosin II known to be important in determining intracellular tension,[33] as well as regulating contraction in smooth muscle through the RhoA/ROCK pathway,[41] demonstrates a modest influence on αSMA expression (Fig. 6 and Supporting Information Fig. S3). At a low 1:1 aspect ratio, blocking myosin II through blebbistatin only shows a slight influence on αSMA expression ($p > 0.05$) on the cyclic peptide, while at high 1:4 aspect ratio, we observe no changes in smooth muscle expression after myosin II inhibition. However, inhibition of ROCK, an upstream effector of myosin, caused marked decreases in α-smooth muscle actin expression at both 1:1 and 1:4 aspect ratios (Fig. 6). While previous studies have highlighted the importance of the Rho/ROCK pathway in the differentiation of MSCs into SMCs,[42] in this study we observe an influence of geometry on ROCK signaling and enhanced smooth muscle phenotype at high aspect ratio. This result supports previous findings of a role for cell shape and stretching in smooth muscle cell proliferation and differentiation.[43,44]

A previous study using patterned MSCs concluded that Rac1 activation rather than RhoA activation is sufficient to induce smooth muscle differentiation.[37] Well-spread MSCs, when activated with TGFβ, underwent SMC differentiation through Rac1 activation. However, the authors used square patterns coated with fibronectin protein. In the present study, we observe that Rac signaling may be guided by both ligand affinity and cell aspect ratio during smooth muscle myogenesis. Unlike the authors of the previous study, we observe a small decrease in αSMA expression after Rac1 inhibition only for MSCs cultured on a high affinity/low aspect ratio combination (cyclic RGD/1:1 aspect ratio). This observation shows how tuning ligand affinity and cell geometry, independently or together, can be used to tune specific signaling pathways toward exploring a desired cellular outcome.

We observe decreases in αSMA expression in all samples treated with an inhibitor of calpain, although changes at a 1:1 aspect ratio were not significantly different from nontreated MSCs. Calpains are a family of calcium-dependent proteases that have been linked to a diverse array of cellular functions including cell motility and focal adhesion turnover.[45,46] They are less studied compared with the Rho GTPases, but have been linked to smooth muscle proliferation[47] as well as mechanosensing.[48] A key feature of the Rho, Rac, and calpain pathways is their involvement in the regulation of focal adhesion complexes and cytoskeletal tension.[49,50] We observe that all three pathways are involved during smooth muscle myogenesis of MSCs as inhibition of any one member appears to alter αSMA expression. However, the involvement of these pathways appears dependent on factors such as ligand affinity and geometry, underscoring the importance of controlling these conditions when studying cellular processes. Central to all three of these signaling molecules is involvement during regulation of focal adhesion dynamics. While we do not measure focal adhesion turnover directly in our study, we investigate changes in the focal adhesion architecture and footprint at an early (24 h, Supporting Information Fig. S2) and late (5 day, Fig. 4) time point. We observe changes in focal adhesion architecture that mirrors changes in smooth muscle actin expression. Interestingly, though we detect differences in overall integrin expression [Fig. 3(c,d)] we observe few differences in integrin localization (Supporting Information Fig. S4). We thereby propose a mechanism where MSC differentiation toward smooth muscle is influenced by several players in regulation of focal adhesion dynamics—Rac, Rho/ROCK, and Calpain—that will be differentially activated under specific contexts of microenvironment stimuli.

Patterning matrix proteins across a material is a powerful tool for the study of cell adhesion and differentiation. Here we present a microcontact printing method using short peptides that allows even greater control over the biophysical and biochemical parameters underlying cell adhesion and associated signaling. We show that even a subtle change in adhesion ligand—a linear versus cyclic peptide—can have significant effects on the behavior of adherent MSCs and lineage specification to a smooth muscle phenotype. Pathway analysis reveals the importance of several mechanotransduction pathways in mediating smooth muscle myogenesis of MSCs. In summary, peptide patterning will allow the investigation of virtually any combination of bioactive peptides, at controlled densities across the biomaterials interface, which may afford spatial control of cellular processes and differentiation outcomes without the need for soluble supplements.

REFERENCES

1. Owens GK. Regulation of differentiation of vascular smooth muscle cells. Physiol Rev 1995;75:487–517.
2. Barry FP, Murphy JM. Mesenchymal stem cells: Clinical applications and biological characterization. Int J Biochem Cell Biol 2004; 36:568–584.

3. Kobayashi M, Inoue K, Warabi E, Minami T, Kodama T. A simple method of isolating mouse aortic endothelial cells. J Atheroscler Thromb 2005;12:138–142.
4. Proudfoot D, Shanahan C. Human vascular smooth muscle cell culture. Methods Mol Biol 2012;806:251–263.
5. Caplan AI. Mesenchymal stem cells. J Orthop Res 1991;9:641–650.
6. McBeath R, Pirone DM, Nelson CM, Bhadriraju K, Chen CS. Cell shape, cytoskeletal tension, and RhoA regulate stem cell lineage commitment. Dev Cell 2004;6:483–495.
7. Kilian KA, Bugarija B, Lahn BT, Mrksich M. Geometric cues for directing the differentiation of mesenchymal stem cells. Proc Natl Acad Sci USA 2010;107:4872–4877.
8. Zhang D, Kilian KA. The effect of mesenchymal stem cell shape on the maintenance of multipotency. Biomaterials 2013;34:3962–3969.
9. Lee J, Abdeen AA, Kim AS, Kilian KA. Influence of biophysical parameters on maintaining the mesenchymal stem cell phenotype. ACS Biomater Sci Eng 2015;1:218–226.
10. Lee J, Abdeen AA, Zhang D, Kilian KA. Directing stem cell fate on hydrogel substrates by controlling cell geometry, matrix mechanics and adhesion ligand composition. Biomaterials 2013;34:8140–8148.
11. Zhang D, Kilian KA. Peptide microarrays for the discovery of bioactive surfaces that guide cellular processes: A single step azide–alkyne "click" chemistry approach. J Mater Chem B 2014;2:4280.
12. Rensen SSM, Doevendans PAFM, van Eys GJJM. Regulation and characteristics of vascular smooth muscle cell phenotypic diversity. Neth Heart J 2007;15:100–108.
13. Gong Z, Niklason LE. Small-diameter human vessel wall engineered from bone marrow-derived mesenchymal stem cells (hMSCs). FASEB J 2008;22:1635–1648.
14. Hellström M, Kalén M, Lindahl P, Abramsson A, Betsholtz C. Role of PDGF-B and PDGFR-beta in recruitment of vascular smooth muscle cells and pericytes during embryonic blood vessel formation in the mouse. Development 1999;126:3047–3055.
15. Hedin U, Thyberg J. Plasma fibronectin promotes modulation of arterial smooth-muscle cells from contractile to synthetic phenotype. Differentiation 1987;33:239–246.
16. Beamish JA, He P, Kottke-Marchant K, Marchant RE. Molecular regulation of contractile smooth muscle cell phenotype: Implications for vascular tissue engineering. Tissue Eng B Rev 2010;16: 467–491.
17. Lozito TP, Kuo CK, Taboas JM, Tuan RS. Human mesenchymal stem cells express vascular cell phenotypes upon interaction with endothelial cell matrix. J Cell Biochem 2009;107:714–722.
18. Kobayashi N, Yasu T, Ueba H, Sata M, Hashimoto S, Kuroki M, Saito M, Kawakami M. Mechanical stress promotes the expression of smooth muscle-like properties in marrow stromal cells. Exp Hematol 2004;32:1238–1245.
19. Kurpinski K, Chu J, Hashi C, Li S. Anisotropic mechanosensing by mesenchymal stem cells. Proc Natl Acad Sci USA 2006;103: 16095–16100.
20. Mrksich M, Whitesides GM. Using self-assembled monolayers to understand the interactions of man-made surfaces with proteins and cells. Annu Rev Biophys Biomol Struct 1996;25:55–78.
21. Love JC, Estroff LA, Kriebel JK, Nuzzo RG, Whitesides GM. Self-assembled monolayers of thiolates on metals as a form of nanotechnology. Chem Rev 2005;105:1103–1169.
22. Wilson K, Stuart SJ, Garcia A, Latour RA. A molecular modeling study of the effect of surface chemistry on the adsorption of a fibronectin fragment spanning the 7-10th type III repeats. J Biomed Mater Res A 2004;69:686–698.
23. Pickford AR, Campbell ID. NMR studies of modular protein structures and their interactions. Chem Rev 2004;104:3557–3566.
24. Hudalla GA, Murphy WL. Using "click" chemistry to prepare SAM substrates to study stem cell adhesion. Langmuir 2009;25:5737–5746.
25. Mas-Moruno C, Rechenmacher F, Kessler H. Cilengitide: The first anti-angiogenic small molecule drug candidate design, synthesis and clinical evaluation. Anticancer Agents Med Chem 2010;10:753–768.
26. Kilian KA, Mrksich M. Directing stem cell fate by controlling the affinity and density of ligand–receptor interactions at the biomaterials interface. Angew Chem Int Ed Engl 2012;51:4891–4895.
27. Kato M, Mrksich M. Using model substrates to study the dependence of focal adhesion formation on the affinity of integrin–ligand complexes. Biochemistry 2004;43:2699–2707.
28. Ruoslahti E. RGD and other recognition sequences for integrins. Annu Rev Cell Dev Biol 1996;12:697–715.
29. Haubner R, Gratias R, Diefenbach B, Goodman SL, Jonczyk A, Kessler H. Structural and functional aspects of RGD-containing cyclic pentapeptides as highly potent and selective integrin α V β 3 antagonists. J Am Chem Soc 1996;118:7461–7472.
30. Lee J, Abdeen AA, Tang X, Saif TA, Kilian KA. Geometric guidance of integrin mediated traction stress during stem cell differentiation. Biomaterials 2015;69:174–183.
31. Parsons JT, Horwitz AR, Schwartz MA. Cell adhesion: Integrating cytoskeletal dynamics and cellular tension. Nat Rev Mol Cell Biol 2010;11:633–643.
32. Morgan MR, Humphries MJ, Bass MD. Synergistic control of cell adhesion by integrins and syndecans. Nat Rev Mol Cell Biol 2007; 8:957–969.
33. Vicente-Manzanares M, Ma X, Adelstein RS, Horwitz AR. Nonmuscle myosin II takes centre stage in cell adhesion and migration. Nat Rev Mol Cell Biol 2009;10:778–790.
34. Amano M, Nakayama M, Kaibuchi K. Rho-kinase/ROCK: A key regulator of the cytoskeleton and cell polarity. Cytoskeleton (Hoboken) 2010;67:545–554.
35. Glading A, Lauffenburger DA, Wells A. Cutting to the chase: Calpain proteases in cell motility. Trends Cell Biol 2002;12:46–54.
36. Goll DE, Thompson VF, Li H, Wei W, Cong J. The calpain system. Physiol Rev 2003;83:731–801.
37. Gao L, McBeath R, Chen CS. Stem cell shape regulates a chondrogenic versus myogenic fate through Rac1 and N-cadherin. Stem Cells 2010;28:564–572.
38. Franco SJ, Huttenlocher A. Regulating cell migration: Calpains make the cut. J Cell Sci 2005;118:3829–3838.
39. Hsiong SX, Ph D, Boontheekul T, Huebsch N, Mooney DJ. Cyclic arginine-glycine-aspartate peptides enhance three-dimensional stem cell osteogenic differentiation. Tissue Eng A 2009;15:263–272.
40. Su JL, Chiou J, Tang CH, Zhao M, Tsai CH, Chen PS, Chang YW, Chien MH, Peng CY, Hsiao M, Kuo ML, Yen ML. CYR61 Regulates BMP-2-dependent osteoblast differentiation through the $\alpha v\beta 3$ integrin/integrin-linked kinase/ERK pathway. J Biol Chem 2010; 285:31325–31336.
41. Somlyo AP, Somlyo AV. Ca2+ sensitivity of smooth muscle and nonmuscle myosin II: Modulated by G proteins, kinases, and myosin phosphatase. Physiol Rev 2003;83:1325–1358.
42. Jeon ES, Park WS, Lee MJ, Kim YM, Han J, Kim JH. A Rho kinase/myocardin-related transcription factor-A-dependent mechanism underlies the sphingosylphosphorylcholine-induced differentiation of mesenchymal stem cells into contractile smooth muscle cells. Circ Res 2008;103:635–642.
43. Thakar RG, Cheng Q, Patel S, Chu J, Nasir M, Liepmann D, Komvopoulos K, Li S. Cell-shape regulation of smooth muscle cell proliferation. Biophys J 2009;96:3423–3432.
44. Ghazanfari S, Tafazzoli-Shadpour M, Shokrgozar MA. Effects of cyclic stretch on proliferation of mesenchymal stem cells and their differentiation to smooth muscle cells. Biochem Biophys Res Commun 2009;388:601–605.
45. Carragher NO, Fincham VJ, Riley D, Frame MC. Cleavage of focal adhesion kinase by different proteases during SRC-regulated transformation and apoptosis. Distinct roles for calpain and caspases. J Biol Chem 2001;276:4270–4275.
46. Yajima Y, Kawashima S. Calpain function in the differentiation of mesenchymal stem cells. Biol Chem 2002;383:757–764.
47. Ariyoshi H, Okahara K, Sakon M, Kambayashi J, Kawashima S, Kawasaki T, Monden M. Possible involvement of m-calpain in vascular smooth muscle cell proliferation. Arterioscler Thromb Vasc Biol 1998;18:493–498.
48. Sedding DG, Homann M, Seay U, Tillmanns H, Preissner KT, Braun-Dullaeus RC. Calpain counteracts mechanosensitive apoptosis of vascular smooth muscle cells in vitro and in vivo. FASEB J 2008;22:579–589.
49. Nobes CD, Hall A. Rho, rac, and cdc42 GTPases regulate the assembly of multimolecular focal complexes associated with actin stress fibers, lamellipodia, and filopodia. Cell 1995;81:53–62.
50. Bhatt A, Kaverina I, Otey C, Huttenlocher A. Regulation of focal complex composition and disassembly by the calcium-dependent protease calpain. J Cell Sci 2002;115:3415–3425.